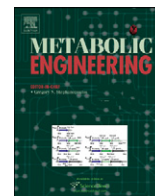


Contents lists available at ScienceDirect

Metabolic Engineering

journal homepage: www.elsevier.com/locate/ymben

Understanding fatty acid synthesis in developing maize embryos using metabolic flux analysis [☆]

Ana Paula Alonso ^{a,b,*}, Val L. Dale ^c, Yair Shachar-Hill ^{a,b}

^a Department of Plant Biology, Michigan State University, East Lansing, MI 48824, USA

^b Great Lakes Bioenergy Research Center, East Lansing, MI 48824, USA

^c Monsanto Calgene Campus, Davis, CA 95616, USA

ARTICLE INFO

Article history:

Received 10 November 2009

Received in revised form

11 February 2010

Accepted 14 April 2010

Keywords:

Zea mays

Metabolic flux analysis

Carbon conversion efficiency

Maize embryo

Fatty acid synthesis

NADP-dependent malic enzyme

ABSTRACT

The efficiency with which developing maize embryos convert substrates into seed storage reserves was determined to be 57–71%, by incubating developing maize embryos with uniformly labeled ¹⁴C substrates and measuring their conversion to CO₂ and biomass products. To map the pattern of metabolic fluxes underlying this efficiency, maize embryos were labeled to isotopic steady state using a combination of labeled ¹³C-substrates. Intermediary metabolic fluxes were estimated by computer-aided modeling of the central metabolic network using the labeling data collected by NMR and GC-MS and the biomass composition. The resultant flux map reveals that even though 36% of the entering carbon goes through the oxidative pentose-phosphate pathway, this does not fully meet the NADPH demands for fatty acid synthesis. Metabolic flux analysis and enzyme activities highlight the importance of plastidic NADP-dependent malic enzyme, which provides one-third of the carbon and NADPH required for fatty acid synthesis in developing maize embryos.

Published by Elsevier Inc.

1. Introduction

Maize (*Zea mays* L) is one of the most important crops in many parts of the world. With starch, fatty acid and protein accumulation in its kernels, it accounts directly and indirectly for a significant portion of the global food supply. In maize kernels, starch synthesis and accumulation mainly occur in the endosperm tissue, whereas fatty acids production takes place predominantly in the embryo (or germ). Empty seed coat experiments have shown that maize kernels mainly receive glucose, fructose and glutamine as sources of carbon and nitrogen (Porter et al., 1985; 1987; Alonso et al., unpublished results). Once in the kernel, these substrates are used by the endosperm and the embryo to generate and accumulate different biomass products, which requires that these two tissues have different patterns of metabolism. Even though starch metabolism has been widely studied and described

in maize endosperm (Glawischnig et al., 2001, 2002; Ettenhuber et al., 2005; Spielbauer et al., 2006; Alonso et al., unpublished results), a number of fundamental questions about fatty acid synthesis in maize embryos remain unresolved, including the routes of carbon flow and the source(s) of reductant and ATP for fatty acid synthesis.

In plants, fatty acid synthesis occurs predominantly in plastids and requires carbon, ATP and reducing power. The carbon source for fatty acid synthesis is in the form of acetyl-coenzyme A (acetyl-CoA) which cannot cross the plastidic membrane (Weaire and Kekwick, 1975; Roughan et al., 1979). Precursors for acetyl-CoA synthesis must thus be generated in the plastid or imported from the cytosol. In heterotrophic oilseeds, lipids can accumulate to relatively high levels, for example, 40% of dry weight in sunflower embryos (Alonso et al., 2007a), and substantial carbon fluxes must enter the plastid to sustain fatty acid biosynthesis. Studies on isolated plastids have demonstrated that a broad range of cytosolic metabolites such as glucose 6-phosphate (glucose 6-P), phosphoenol pyruvate (PEP), pyruvate and malate are capable of supporting fatty acid synthesis (Smith et al., 1992; Kang and Rawsthorne, 1994, 1996; Qi et al., 1995; Eastmond and Rawsthorne, 2000; Pleite et al., 2005). These can be taken up and utilized for fatty acid synthesis at different rates by plastids from various plant tissues, species and stages of development.

Fatty acid synthesis also depends upon supplies of ATP and reducing power. In green seeds, light energy can be used by chloroplasts to generate ATP and NADPH (Browse and Slack,

Abbreviations: Acetyl-CoA, Acetyl-coenzyme A; DAP, Days after pollination; CCE, Carbon conversion efficiency; GABA, Gamma-aminobutyric acid; GC, Gas chromatography; MS, Mass spectrometry; NMR, Nuclear magnetic resonance; OPPP, Oxidative pentose-phosphate pathway; -P, -phosphate; PEP, Phosphoenolpyruvate; PEG, Polyethylene glycol; TAG, Triacyl glycerol; TCA, Tricarboxylic acid; RuBisCo, Ribulose-1,5-bisphosphate carboxylase oxygenase

[☆]Funding for this work was provided by Rennessen PLC and the Great Lakes Bioenergy Research Center (DOE BER Office of Science DE-FC02-07ER64494).

* Corresponding author at: Department of Plant Biology, Michigan State University, East Lansing, MI 48824, USA. Fax: +1 517 353 1926.

E-mail address: alonsoa@msu.edu (A. Paula Alonso).

1096-7176/\$ - see front matter Published by Elsevier Inc.
doi:10.1016/j.ymben.2010.04.002

Please cite this article as: Paula Alonso, A., et al., Understanding fatty acid synthesis in developing maize embryos using metabolic flux analysis. *Metab. Eng.* (2010), doi:10.1016/j.ymben.2010.04.002

1985; Ruuska et al., 2004; Schwender et al., 2004, 2006; Goffman et al., 2005), whereas plastids isolated from heterotrophic tissues must either generate these compounds internally or import them from the cytosol (Browse and Slack, 1985; Hill and Smith, 1991; Smith et al., 1992; Kleppinger-Sparace et al., 1992; Neuhaus et al., 1993; Kang and Rawsthorne, 1996). The ATP necessary for fatty acid synthesis in non-photosynthetic tissues can be produced inside the plastid during the synthesis of acetyl-CoA from glucose 6-P and PEP (Boyle et al., 1990; Kleppinger-Sparace et al., 1992; Qi et al., 1994). However the uptake of ATP from the cytosol has been shown to have a critical role in fatty acid synthesis since it maintains optimal rates of fatty acid synthesis on isolated plastids (Fuhrmann et al., 1994; Möhlmann et al., 1994; Qi et al., 1994). Besides ATP, fatty acids synthesis also requires large amounts of reducing equivalents in the form of NADH and NADPH. It was proposed that, in isolated plastids from heterotrophic tissues, reducing power could be generated via the conversion of imported malate into acetyl CoA; one mole of NADPH is liberated during the reaction catalyzed by plastidic NADP-dependent malic enzyme (EC 1.1.1.40) and one mole of NADH by pyruvate dehydrogenase (Smith et al., 1992; Pleite et al., 2005). Reductant can also be generated by the OPPP where imported glucose 6-P is oxidized to stimulate fatty acid synthesis in isolated plastids (Kang and Rawsthorne, 1996).

In vitro studies on isolated plastids have led to valuable information such as determining the possible routes of carbon for fatty acid synthesis and the potential sources of reductant and ATP (Neuhaus and Emes, 2000; Rawsthorne, 2002), but their results do not necessarily reflect what happens *in vivo*. For instance, Pleite et al. (2005) showed that when different carbon sources were supplied to plastids isolated from developing sunflower embryos, malate supported the highest rates of fatty acid synthesis throughout the period of oil accumulation. Later, metabolic flux analysis performed in developing sunflower embryos revealed that malate is a minor source of carbon and plastidic NADP-dependent malic enzyme is an insignificant source of reductant for fatty acid synthesis (Alonso et al., 2007a). Indeed, metabolic flux analysis, which provides a detailed understanding of metabolism during seed development, has been recently used to study metabolism in whole embryos *in vivo* (Schwender et al., 2006; Sriram et al., 2004; Alonso et al., 2007a; Allen et al., 2009a; Lonien and Schwender, 2009). In the present study we have applied metabolic flux analysis to quantify the flow of carbon through the primary metabolic network (Ratcliffe and Shachar-Hill, 2005, 2006; Dieuaide-Noubhani et al., 2007; Libourel and Shachar-Hill, 2008; Allen et al., 2009b) in developing maize embryos during oil accumulation to better understand fatty acid synthesis in this tissue. We resolve a number of fundamental metabolic issues, including the sources of reductant and ATP for fatty acid synthesis and the degree to which cytosolic, plastidic and mitochondrial metabolic fluxes are integrated in developing maize embryos. Lastly, this study points to the importance of NADP-dependent malic enzyme for fatty acid synthesis in developing maize embryos.

2. Materials and methods

2.1. Labeled isotopes

[U-¹⁴C₆]glucose (317 mCi/mmol) and [U-¹⁴C₅]glutamine (242 mCi/mmol) were from Amersham Biosciences (Piscataway, NJ). [U-¹⁴C₆]fructose (248 mCi/mmol) was from Moravex (Brea, CA). [1-¹³C₁]glucose and [U-¹³C₅]glutamine were from Isotec (Miamiasburg, OH). [2-¹³C₁]glucose was from Cambridge Isotope Laboratories, Inc. (Andover, MA).

2.2. Plant material

Maize plants (*Zea mays* L.) line LH59 were grown in 30-cm pots in a greenhouse maintained at 30–31 °C/20–21 °C day/night temperature and with supplemental lighting to provide irradiance of ~900–1400 μE m⁻² s⁻¹ and a 18/06 h day/night photoperiod. Plants were hand pollinated and the ears were detached at 15 days after pollination (DAP) and taken to a laminar flow bench for dissection.

2.3. Medium composition and embryo culture conditions

The maize ear was sprayed with isopropanol and flamed. After aseptically removing the inner husks and silks, the developing embryos were dissected under aseptic conditions and transferred into the following culture medium. Carbon and nitrogen medium sources were: glucose (200 mM), fructose (200 mM) and glutamine (40 mM). The minerals were provided by 4.3 g L⁻¹ MS basal salts. Polyethylene glycol (PEG) 4000 was added at 10% to adjust osmotic potential. The vitamin additions were (μg mL⁻¹): nicotinic acid, 5; pyridoxin hydrochloride, 0.5; thiamine hydrochloride, 0.5; folic acid, 0.5, respectively. MES 10 mM was included as a buffer and the medium adjusted to pH 5.8 with 1 N potassium hydroxide. The embryos were placed on double-glass fiber filters soaked with 8 mL of the medium previously described and cultured for 7 days at 25 °C in the dark in a petri dish or a 250 mL screw-cap Erlenmeyer flask sealed with a septum closure.

2.4. Determination of O₂ consumption and CO₂ production

Immediately after culture, the flasks were placed in an ice bath and 1 mL 0.2 N hydrochloric acid was injected through the septum to stop metabolism and to release inorganic carbon to the flask headspace. Duplicate 200 μL gas samples were withdrawn from the flask headspace using a 1 mL syringe, and injected into an InfraRed Gas Analyzer (IRGA) to determine total CO₂ production and a paramagnetic oxygen analyzer to measure total O₂ consumption as previously described by Allen et al. (2009a).

2.5. Separation of biomass compounds

After incubation, embryos were removed and rinsed three times each with 10 mL water to remove surface labeling. The embryos were then frozen with liquid nitrogen and lyophilized. Compounds (oil, proteins and cell wall) were extracted as described by Goffman et al. (2005) with modifications reported by Alonso et al. (2007a). Starch was extracted from the residue of protein extraction as described by Moing et al. (1994).

Oil composition was determined by gas chromatography (GC) with flame ionization detection of Fatty Acid Methyl Esters (FAMES) as described by Goffman et al. (2005). Amino acids from protein hydrolysis were derivatized with *o*-phthalaldehyde, separated on a reverse phase system and quantified as described by Schuster (1988).

2.6. Calculation of carbon uptake, balance and carbon conversion efficiency

As described by Goffman et al. (2005), the CO₂ was trapped and ¹⁴CO₂ present in the trapping solution was counted. Glucose, fructose and glutamine uptake were estimated from labeling experiments in which [U-¹⁴C₆]glucose, [U-¹⁴C₆]fructose or [U-¹⁴C₅]glutamine were supplied, by dividing the total ¹⁴C incorporated by developing maize embryos and ¹⁴CO₂ released by the specific radioactivity of the substrates added to the medium. Calculation of carbon balance and carbon conversion

efficiency (CCE) was determined according to Goffman et al. (2005) by providing all carbon sources uniformly ^{14}C -labeled at the same specific activity and determining ^{14}C incorporation into biomass end products and released as $^{14}\text{CO}_2$.

2.7. Nuclear magnetic resonance (NMR) analyses

Spectra were acquired at 25 °C with a Varian 600 MHz spectrometer equipped with a 5 mm probe. The oil extract was resuspended in 600 μL deuteriochloroform (CDCl_3) and ethanol soluble compounds and starch fraction in deuterium oxide (D_2O). ^1H NMR spectra were obtained at 599.85 MHz with a pulse of 11.5 μs (corresponding to an angle of 90°) using a recycling time greater than $6T_1$. ^{13}C NMR spectra were obtained at 150.84 MHz with a pulse of 8.0 μs (corresponding to an angle of 90°) using a recycling time greater than $6T_1$. The absolute ^{13}C enrichments were determined as described by Rontein et al. (2002).

2.8. GC-MS analyses of protein hydrolysates

Proteins were hydrolyzed in 6N hydrochloric acid and the amino acids were derivatized to N,O-*tert*-butyldimethylsilyl (TBDMS) derivatives as described previously (Schwender et al., 2003). TBDMS-amino acids were analyzed in GC-MS. The systems used are Agilent Technologies 5973N Inert Mass Selective detector instruments, a G2578A system with a 30×0.25 mm HP5 column (from Hewlett Packard) and a G2589A system with a 60×0.25 mm DB5MS column (from J&W Scientific). The carrier gas was helium at a flow rate of 1 mL/min. The relative abundances of mass isotopomers in selected fragments of each analyzed derivative were measured using selected ion monitoring (Schwender et al., 2003). Correction for the occurrence of ^{13}C in derivative parts of the molecules and for heavy isotopes in heteroatoms (C, H, O, N, Si) at their natural abundances was performed as described earlier (Schwender et al., 2003).

2.9. Modeling metabolic pathways

The metabolic model (Fig. 3) described in Supplemental Table 2 was programmed in the 13C-FLUX format (Wiechert et al., 2001). In order to include data from the three separate experiments with [$1\text{-}^{13}\text{C}_1$]glucose, [$2\text{-}^{13}\text{C}_1$]glucose and [$\text{U-}^{13}\text{C}_5$]glutamine into a single flux estimation procedure, each flux and metabolite pool was programmed three times (using subscript 2 for the [$2\text{-}^{13}\text{C}_1$]glucose experiment, and U for the [$\text{U-}^{13}\text{C}_5$]glutamine experiment). Equality of identical fluxes in the separate metabolic networks thus defined was forced by using equality equations. The following net fluxes Vg, Vf, Va, Vfas2, Valdp, Vfas1, Vppp1, Vme, Vpepc, Vwall and Vsta (for expansion, please see Supplemental Table 2) were set free, whereas fluxes through amino acid synthesis were constrained to their experimental values. The exchange fluxes named Vhk1, Vgf, Vald, Vgl, Vhcp, Vtcp, Vppp2, Vppp3, Vppp4, Vfum1 and Vpepc were set as free, whereas Vhk2, Vglyco, Vfas2a, Vfas2b, Vpk, Vpyr, Vstsp, Valpd, Vglycp, Vpkp, Vpdhp, Vmep, Vppp1, Vpdh, Vcs, Vca, Vsfa, Vme and the exchange fluxes of amino acid synthesis were constrained to 0 (irreversible). Flux values quantified by biomass composition and quantification (Vfas2, Vfas1, Vwall and Vsta) as well as the rate of substrate uptake (Vg, Vf and Va) were included as measurements in the 13C-FLUX model. The percentage of ^{13}C enrichments measured by ^1H and ^{13}C NMR and the abundance of mass isotopomers obtained by GC-MS from the three different labeling experiments were entered as labeling measurements in the model. The optimization program used was Donlp2 with over 1500 different starting points. The results are presented in Fig. 3 and Table 2.

2.10. In vitro enzyme activities

Enzyme activities were measured in extracts obtained from five 22DAP endosperms or ten 22DAP germs. Frozen tissues were ground to fine powder in liquid nitrogen in a pre-chilled mortar and homogenized with 100 mM Hepes buffer (pH 7.5) containing 5 mM magnesium chloride and 1 mM dithiothreitol. The homogenates were centrifuged at 4 °C for 5 min at 1300g. The supernatants were immediately assayed for enzyme activities; the absorbance at 342 nm was monitored at 27 °C with a DU® spectrophotometer (Beckman Coulter).

The activity of 6-phosphogluconate dehydrogenase (EC 1.1.1.43) was measured by incubating the extract with 800 μL of 100 mM Hepes assay buffer (pH7.5) containing 10 mM magnesium chloride, 50 μL NADP 20 mM and 100 μL 6-phosphogluconate 10 mM. Then glucose 6-P dehydrogenase (EC 1.1.1.49) activity was monitored after adding 100 μL glucose 6-P 30 mM.

Malic enzyme activities (EC 1.1.1.40) were monitored by incubating the extract with 800 μL of 100 mM Hepes assay buffer (pH7.5) containing 10 mM magnesium chloride, 100 μL malate 40 mM and 50 μL NADP 20 mM or 50 μL NAD 20 mM for NADP-dependent or NAD-dependent forms, respectively.

3. Results

3.1. Maize embryos culture

According to “empty seed coat” experiments performed on maize kernels *in planta* (Porter et al., 1985, 1987) and in culture (Alonso et al., unpublished results), maize kernels mainly receive glucose, fructose and glutamine as source of carbon and nitrogen. Glucose, fructose and glutamine were used with a respective concentration of 200, 200 and 40 mM with 10% PEG in order to cultivate maize embryos *in vivo*. Under these conditions, the cultured embryos accumulate dry weight at a rate of 1.08 ± 0.16 mg embryo $^{-1}$ day $^{-1}$. This is not significantly different from the growth rate *in planta* (1.06 ± 0.03 mg embryo $^{-1}$ day $^{-1}$). Fatty acid composition in cultured maize embryos was also similar to that of embryos developing *in planta*, with the cultured embryos having somewhat more alpha linoleic acid (C18:2) and less linoleic acid (C18:1) than the embryos growing *in planta*; the percentage of total fatty acid (w/w) was not significantly different (Fig. 1).

3.2. Carbon conversion efficiency (CCE)

Uniformly labeled ^{14}C substrates were supplied and carbon balance was determined in developing maize embryos by measuring ^{14}C incorporated into biomass compounds (starch, oil, proteins and cell wall) and $^{14}\text{CO}_2$ produced. Fig. 2A presents the partitioning of the ^{14}C carbon after labeling with [$\text{U-}^{14}\text{C}_6$]glucose, [$\text{U-}^{14}\text{C}_6$]fructose and [$\text{U-}^{14}\text{C}_5$]glutamine for 7 days (from 15DAP to 22DAP); $18.0 \pm 1.2\%$, $2.1 \pm 0.3\%$, $9.6 \pm 0.2\%$ and $8.5 \pm 0.6\%$ of the ^{14}C was incorporated into oil, protein, starch and cell wall, respectively, which represents a CCE of between 57% and 71% (depending on whether the low molecular weight soluble fraction is considered as part of the biomass).

3.3. Metabolic fluxes in developing maize germs

3.3.1. Carbon uptake

Glucose, fructose and glutamine uptakes were determined after incubating maize embryos with medium containing [$\text{U-}^{14}\text{C}_6$]glucose, [$\text{U-}^{14}\text{C}_6$]fructose or [$\text{U-}^{14}\text{C}_5$]glutamine for 7 days and then dividing the total ^{14}C incorporated into developing

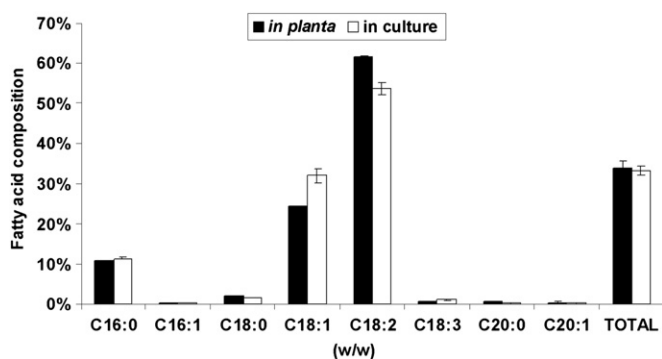


Fig. 1. Fatty acid composition in developing maize embryos. Fatty acid composition was determined as described in Materials and methods section on maize embryos harvested from the plant at 22DAP and embryos cultivated from 15DAP to 22DAP. Errors bars represent standard deviations of 3 independent experiments.

maize embryos and $^{14}\text{CO}_2$ released by the specific radioactivity of the medium. Glucose, fructose and glutamine uptake rates were found to be 291 ± 32 , 340 ± 27 and 55 ± 3 nmol h^{-1} embryo $^{-1}$, respectively.

3.3.2. Biomass accumulation

Oil, starch and cell wall accumulation was estimated according to the biomass composition determined by ^{14}C -balance (Fig. 2B) and embryo growth. The rates of oil, starch and cell wall syntheses were found to be 491 ± 104 , 89 ± 16 and 79 ± 15 nmol h^{-1} embryo $^{-1}$, respectively.

3.3.3. ^{13}C -labeling

Isotopic steady state was confirmed by incubating maize embryos with 100% $[1-^{13}\text{C}_1]\text{glucose}$ for 7 and 11 days. The labeling did not increase between 7 and 11 days, showing that isotopic steady state is reached within 7 days of labeling (data not shown).

Maize embryos were thus grown for 7 days in the culture medium described above (Section 3.1) using three separate labeling experiments: 100% $[1-^{13}\text{C}_1]\text{glucose}$ ($n=3$), 100% $[2-^{13}\text{C}_2]\text{glucose}$ ($n=3$) and 100% $[U-^{13}\text{C}_5]\text{glutamine}$ ($n=2$). The combination of different labeling experiments is common when performing metabolic flux analysis in plant seeds (Schwender et al., 2006; Alonso et al., 2005, 2007a; Libourel et al., 2007; Allen et al., 2009a) because it allows a better definition of the metabolic network; $[1-^{13}\text{C}_1]\text{glucose}$ gives information on the glycolysis/reversibility of the glycolysis, $[2-^{13}\text{C}_2]\text{glucose}$ on the OPPP and $[U-^{13}\text{C}_5]\text{glutamine}$ on the TCA cycle. After extraction, the ^{13}C enrichment of oil, starch and soluble metabolites was determined by ^1H and ^{13}C -NMR (Table 1), proteins were extracted, hydrolyzed, derivatized and the relative abundance of mass isotopomers was determined by GC-MS (Supplement 1).

3.3.4. Modeling

The model of central metabolic pathways for developing maize embryos was built according to information available in the literature about other heterotrophic plant tissues (Dieuaid-Noubhani et al., 1995; Rontein et al., 2002; Alonso et al., 2007a; 2007b; unpublished results; Williams et al., 2008) and the labeling data we collected (Table 1, Supplement 1). The substantial loss of label at carbon 1 (C1) of starch glucosyl unit compared to the labeling of sucrose glucosyl unit after labeling with $[1-^{13}\text{C}_1]\text{glucose}$ (Table 1) indicates not only the operation of the OPPP but also its localization in the plastid. The significant difference observed between the enrichments of sucrose glucosyl and fructosyl units after a labeling with $[1-^{13}\text{C}_1]\text{glucose}$ or

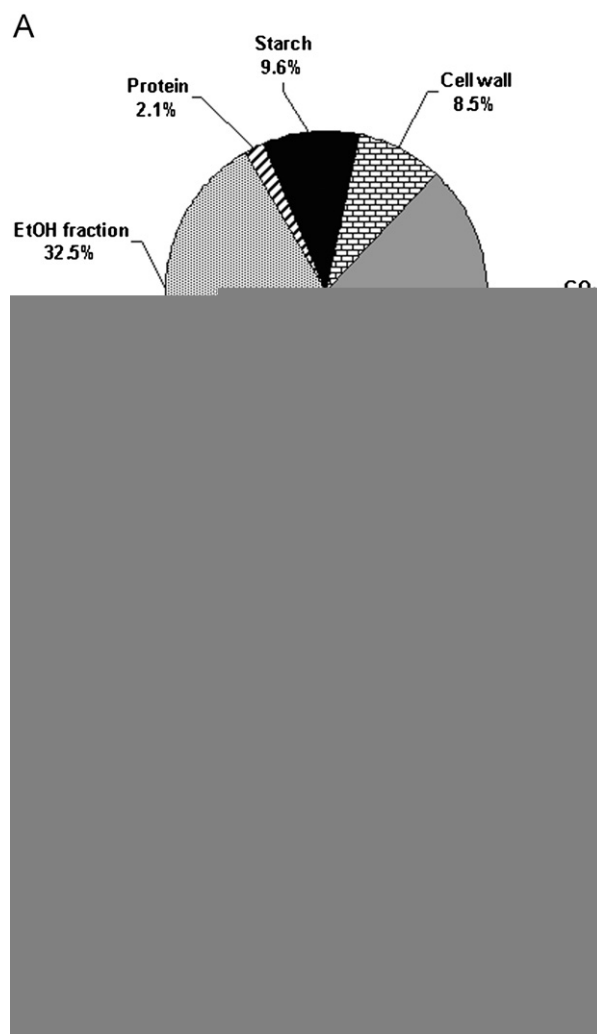


Fig. 2. Carbon allocation in maize embryos. (A) Distribution of ^{14}C -labeling among biomass fractions and CO_2 . Maize embryos were cultured at 27 °C for 7 days in the presence of $[U-^{14}\text{C}_6]\text{glucose}$, $[U-^{14}\text{C}_6]\text{fructose}$ and $[U-^{14}\text{C}_6]\text{glutamine}$. After culture, the $^{14}\text{CO}_2$ was collected by flushing the flasks through a trapping system as described by Goffman et al. (2005). Embryos were frozen in liquid N_2 and the analysis of ^{14}C -labeling in biomass components was then performed as described in Materials and methods section. (B) Biomass composition in maize embryos. The percentage of dry weight for each biomass compound was deducted according to the percentage of ^{14}C -balance and estimating that molC/mol TAG, molC/mol amino acid and molC/mol carbohydrate is, respectively, 60.7, 4.8 and 6 and that molecular weight of TAG, average amino acid and glucosyl unit is, respectively, 933.6, 110.4 and 162.

$[2-^{13}\text{C}_1]\text{glucose}$ (Table 1) indicates that cytosolic hexose-P are not rapidly exchanged. The enrichment of the C1 of sucrose glucosyl unit is lower than glucose C1 after labeling with $[1-^{13}\text{C}_1]\text{glucose}$ (Table 1), revealing a net flux from fructose-6P to glucose-6P. Furthermore, the enrichment of glucose C1 (Table 1) is diluted compared to external 100% $[1-^{13}\text{C}_1]\text{glucose}$, indicating the formation of glucose from glucose 6-P via a potential glucose 6-phosphorylase or via sucrose synthesis and degradation cycle (Alonso et al., 2005). After labeling with $[U-^{13}\text{C}_5]\text{glutamine}$, we did not detect significant labeling in starch glucosyl or sucrose glucosyl units (Table 1), showing the absence of significant gluconeogenic flux. Nevertheless, acetyl-CoA units of fatty acids were significantly enriched after labeling with $[U-^{13}\text{C}_5]\text{glutamine}$ (Table 1), which indicates that plastidic NADP-dependant malic enzyme can be a significant route for fatty acid synthesis in maize embryos. NAD-dependent malic enzyme and the PEP carboxylase

Table 1Steady-state ^{13}C enrichments of maize embryo metabolites after labeling with 100% $[1-^{13}\text{C}_1]$ glucose, 100% $[U-^{13}\text{C}_6]$ glucose or 100% $[U-^{13}\text{C}_5]$ glutamine.

Metabolite	Carbon	Cumomer	Labeling data (% ^{13}C enrichment)		
			$[1-^{13}\text{C}_1]$ Glucose	$[2-^{13}\text{C}_1]$ Glucose	$[U-^{13}\text{C}_5]$ Glutamine
AcetylCoA unit of fatty acid	1	1x	4.87 ± 1.08	13.34 ± 1.93	5.98 ± 1.61
	2	x1	15.62 ± 0.83	2.97 ± 0.95	5.74 ± 1.34
Starch glucosyl unit	1	1xxxxx			1.63 ± 0.79
		11xxxx		0.29 ± 0.48	
		10xxxx	29.48 ± 1.81	6.00 ± 1.07	
	2	110xxx+011xxx		1.13 ± 0.64	
		010xxx	2.35 ± 0.94	1.06 ± 0.83	
	3	x110xx+x011xx		0.89 ± 0.53	
		x010xx	2.60 ± 1.02	3.64 ± 1.01	
	4	xx110x+xx011x		0.19 ± 0.40	
		xx010x	1.56 ± 0.34	1.69 ± 0.51	
	5	xxx110+xxx011		0.42 ± 0.39	
		xxx010	1.32 ± 0.58	8.41 ± 0.78	
	6	xxxx01	9.83 ± 1.38	2.35 ± 0.39	
Sucrose glucosyl unit	1	1xxxxx			1.37 ± 0.61
		11xxxx	0.87 ± 6.61	0.61 ± 0.26	
		10xxxx	39.95 ± 0.30	3.73 ± 1.56	
	2	010xxx		41.65 ± 1.28	
		11xxxx	0.59 ± 0.55		
	3	01xxxx	2.68 ± 3.39		
		x110xx+x011xx		1.07 ± 0.30	
	4	x010xx	2.54 ± 0.58	2.59 ± 0.34	
		xx110x+xx011x		0.94 ± 1.00	
	5	xx010x	1.71 ± 0.67	2.53 ± 1.57	
		xxx010	2.03 ± 1.00	6.53 ± 0.54	
	6	xxxx01	7.15 ± 0.98	1.24 ± 1.20	
Sucrose fructosyl unit	1	1xxxxx		2.03 ± 1.91	
		10xxxx	18.79 ± 2.88		
		110xxx+011xxx		0.89 ± 0.34	
	2	010xxx	1.96 ± 1.93	16.46 ± 1.16	
		11xxxx		0.59 ± 0.35	
	3	01xxxx	2.68 ± 3.39		
		x110xx+x011xx		1.72 ± 0.28	
	4	x010xx	1.64 ± 0.54	1.72 ± 0.28	
		xx010x	1.21 ± 0.48	3.83 ± 1.97	
	5	xxxx1x		4.49 ± 0.60	
		xxx010	1.08 ± 0.67		
	6	xxxx01	4.67 ± 0.68	1.18 ± 1.10	
Glutamine	2	111xx			6.14 ± 4.08
		010xx	5.45 ± 1.46	9.52 ± 3.49	
	3	x111x			48.17 ± 1.69
		x011x+x110x			10.27 ± 0.71
	4	x010x	4.47 ± 1.03	11.56 ± 3.34	3.31 ± 3.75
		xx111			49.09 ± 0.51
	xx010	9.92 ± 0.62	7.81 ± 0.72		
Glucose	1	1xxxxx	73.28 ± 3.90		
Glycerol unit of TAG	3	1xx+xx1	6.90 ± 1.70		
Alanine	2	010	0.03 ± 0.02	0.21 ± 0.02	0.01 ± 0.00
	3	x01	0.20 ± 0.02	0.03 ± 0.01	
		x11			0.01 ± 0.00
GABA	2	010x	0.23 ± 0.01	0.04 ± 0.01	
	3	x010	0.10 ± 0.01	0.07 ± 0.01	
	4	xx01	0.10 ± 0.01	0.07 ± 0.00	

Maize embryos were incubated for 7 days in the presence of 100% $[1-^{13}\text{C}_1]$ glucose, 100% $[2-^{13}\text{C}_1]$ glucose or 100% $[U-^{13}\text{C}_5]$ glutamine. Oil fraction, sugars, amino acids and starch were extracted as described in Materials and Methods section and then analyzed by ^1H and ^{13}C -NMR. The ^{13}C enrichment value (in %) of each carbon was calculated and reported below as an average of two (for the 100% $[U-^{13}\text{C}_5]$ glutamine labelings) or three experiments (for the 100% $[1-^{13}\text{C}_1]$ glucose and 100% $[2-^{13}\text{C}_1]$ glucose labeling). 0.0025 was added to all SD's to account for potential instrument errors and to prevent small experimental SD's from biasing the fitting process since SD's of small sample sets are poor estimates of true population SD's. Cumomers are described by series of "x", "1" and "0", each one representing an atom of carbon of the molecule. "x", undetermined; "1", labeled; "0", unlabeled.

are the only two reactions that are potentially active between the malate/oxaloacetate and PEP/pyruvate pools. All the information described above about compartmentalization as well as the presence or absence of reactions was included in the model described in Supplemental Table 2.

^{13}C -FLUX software (Möllney et al., 1999; Wiechert and de Graaf, 1997; Wiechert et al., 1997, 1999) was used for quantifying the flux values. The following information was entered in the model: (i) the labeling data obtained from the 3 different labeling experiments (100% $[1-^{13}\text{C}_1]$ glucose, 100% $[2-^{13}\text{C}_1]$ glucose and

100% [U-¹³C₅]glutamine; $n=8$ total); (ii) reactions describing carbon metabolism; (iii) rates of glucose, fructose and glutamine uptake determined by ¹⁴C-labeling experiments; and (iv) rates of biomass accumulated during 7 days of culture and biomass composition data. This information allowed flux values to be estimated and confidence intervals determined. The resulting flux map and the values of net and exchange fluxes are shown in Fig. 3 and Table 2.

3.3.5. Model validation

To avoid incorrect flux estimates due to local minima in the fitting process, the optimization procedure was repeated over 1500 times with different initial flux values. The best fit was also the most commonly optimized set of values (over 90% of the fits). We compared the CCE determined directly from ¹⁴C experiments (57–71%; Fig. 2), to the one determined from the flux map (Fig. 3) which is 62–69%. The agreement between the two supports the validity of the flux map since this was determined without reference to the ¹⁴C data used for the CCE measurement. We further validated the modeling results by comparing the rate of CO₂ production determined from the rates of substrate uptake and the percentage of ¹⁴CO₂ determined in ¹⁴C-labeling experiments (1190 ± 108 nmol h⁻¹ embryo⁻¹) to the rate determined from the model (1183 ± 64 nmol h⁻¹ embryo⁻¹, Table 2). Finally, the ability of the model to explain the experimental data is shown in Fig. 4 where simulated data are plotted against measured labeling data. The fact that this distribution is close to a 1:1 linear relationship with a high correlation coefficient indicates that the

mathematical flux model describes the experimentally observed data well.

3.4. Source of carbon and reducing power for fatty acid synthesis

Based on the analysis of the labeling results (Fig. 3; Table 2), approximately 70% of the carbon for fatty acid synthesis is derived from PEP produced from hexose-P imported into the plastid (Fig. 5). The remaining 30% of the carbon for fatty acid synthesis comes from the import of malate into the plastid. Thus, even though the majority of the carbon enters the plastid at the level of hexose-P, malate remains a significant source of carbon for plastidic fatty acid synthesis during maize embryo development (Fig. 5). The oxidative part of the pentose-P pathway does not provide enough reductant for oil production. The estimated OPPP flux produces 416 nmol NADPH h⁻¹ embryo⁻¹, whereas fatty acid synthesis requires 547 nmol NADPH h⁻¹ embryo⁻¹. The flux through plastidic NADP-dependant malic enzyme provides 163 nmol NADPH h⁻¹ embryo⁻¹, which meets the remaining demand for NADPH production (Fig. 5). Plastidic glyceraldehyde 3-P dehydrogenase and pyruvate dehydrogenase provide a total of 946 nmol NADH h⁻¹ embryo⁻¹, which is more than sufficient for fatty acid synthesis, which requires only 547 nmol NADH h⁻¹ embryo⁻¹ (Fig. 5). Plastidic pyruvate kinase and phosphoglycerate kinase produce 792 nmol ATP h⁻¹ embryo⁻¹ while fatty acid synthesis needs 547 nmol ATP h⁻¹ embryo⁻¹ (Fig. 5).

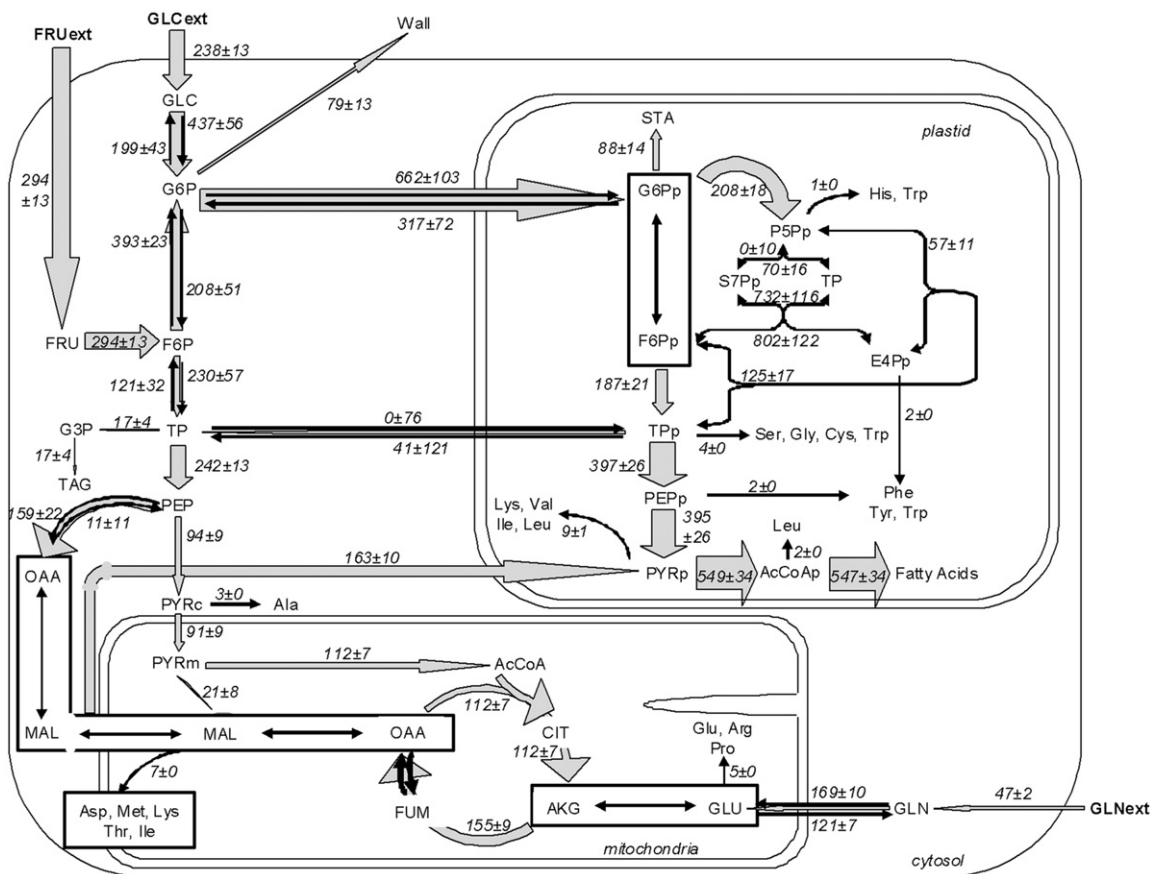


Fig. 3. Metabolic network and fluxes in maize embryos. The scheme shown is a simplified overview indicating steps for which our model allows calculations of fluxes and their localization. Values reported are the best fit and the ones most commonly obtained by optimized fitting. Units are nmol molecule h⁻¹ embryo⁻¹ ± confidence interval. For the net fluxes, gray arrow widths are directly proportional to flux values. The boxes surrounding metabolites indicate that any differences in the labeling between these metabolites cannot be distinguished by our experiments.

Table 2
Metabolic fluxes in maize embryos.

Flux name	Flux or rate description	Flux values (nmol h ⁻¹ embryo ⁻¹)	
		Net	Exchange
Vg	Rate of glucose uptake	238 ± 13 ^a	0 ^b
Vf	Rate of fructose uptake	294 ± 13 ^a	0 ^b
Va	Rate of glutamine uptake	47 ± 2 ^a	0 ^b
Vhk1	Flux through hexokinase from glucose to G6P	238 ± 13 ^c	197 ± 35 ^c
Vhk2	Flux through hexokinase from fructose to F6P	294 ± 13 ^c	0 ^b
Vgf	Fluxes catalyzed by G6P isomerase	-185 ± 28 ^c	393 ± 15 ^c
Vald	Fluxes catalyzed by cytosolic aldolase	109 ± 25 ^c	121 ± 28 ^c
Vglyco	Glycolytic flux in the cytosol	242 ± 13 ^c	0 ^b
Vfas2	Rate of glycerol incorporation into TAG	17 ± 4 ^a	0 ^b
Vpk	Flux catalyzed by pyruvate kinase	94 ± 9 ^c	0 ^b
Vpyr	Flux of pyruvate from cytosol to mitochondria	91 ± 9 ^c	0 ^b
Vgl	Flux of glutamine to glutamate	47 ± 2 ^c	121 ± 6 ^c
Vhcp	Exchange of cytosolic and plastidic hexose-P	345 ± 31 ^c	317 ± 52 ^c
Vstsp	Starch synthesis from plastidic hexose-P	88 ± 14 ^c	0 ^c
Valdp	Fluxes catalyzed by plastidic aldolase	187 ± 21 ^c	0 ^b
Vglycp	Glycolytic flux in the plastid	397 ± 26 ^c	0 ^b
Vpkp	Flux catalyzed by plastidic pyruvate kinase	395 ± 26 ^c	0 ^b
Vpdhp	Flux catalyzed by plastidic pyruvate DH	549 ± 34 ^c	0 ^b
Vfas1	Flux of AcCoA to fatty acid synthesis	547 ± 34 ^a	0 ^b
Vmep	Flux catalyzed by plastidic malic enzyme	163 ± 10 ^c	0 ^b
Vtcp	Exchange of cytosolic and plastidic triose-P	-41 ± 45 ^c	0 ± 86 ^c
Vppp1	Flux of the oxidative part of the pentose-P pathway	208 ± 18 ^c	0 ^b
Vppp2	Fluxes catalyzed by transketolase	70 ± 6 ^c	0 ± 10 ^c
Vppp3	Fluxes catalyzed by transaldolase	70 ± 6 ^c	732 ± 58 ^c
Vppp4	Fluxes catalyzed by transketolase	68 ± 6 ^c	57 ± 10 ^c
Vpdh	Flux catalyzed by pyruvate DH	112 ± 7 ^c	0 ^b
Vcs	Flux through citrate synthase	112 ± 7 ^c	0 ^b
Vca	Flux catalyzed by aconitase	112 ± 7 ^c	0 ^b
Vsfa	Flux through 2-oxoglutarate DH	155 ± 9 ^c	0 ^b
Vfum	Flux catalyzed by fumarase	156 ± 10 ^c	high exchange ^c
Vme	Flux through malic enzyme	21 ± 8 ^c	0 ^b
Vpepc	Anaplerotic flux through PEPc	148 ± 11 ^c	11 ± 11 ^c
Vco2	Rate of CO ₂ production	1183 ± 64 ^c	0 ^b
Vwall	Rate of wall synthesis	79 ± 13 ^a	0 ^b
Vsta	Total starch synthesis	88 ± 14 ^a	0 ^b
Vp5peff	Flux of P5Pp to amino acids for protein synthesis	1 ± 0 ^a	0 ^b
Vtpeff	Flux of TP to amino acids for protein synthesis	4 ± 1 ^a	0 ^b
Vpepeff	Flux of PEP to amino acids for protein synthesis	2 ± 1 ^a	0 ^b
Ve4peff	Flux of E4Pp to amino acids for protein synthesis	2 ± 0 ^a	0 ^b
Vpyrpeff	Flux of PYRp to amino acids for protein synthesis	9 ± 1 ^a	0 ^b
VAcCoApeff	Flux of AcCoAp to amino acids for protein synthesis	2 ± 0 ^a	0 ^b
Vpyrceff	Flux of PYRc to amino acids for protein synthesis	3 ± 0 ^a	0 ^b
Voaeff	Flux of OAA to amino acids for protein synthesis	7 ± 0 ^a	0 ^b
Vglueff	Flux of GLU to amino acids for protein synthesis	5 ± 0 ^a	0 ^b

Fluxes units are nmol molecule h⁻¹ embryo⁻¹. The rates of glucose (Vg), fructose (Vf) and glutamine (Va) uptake were determined as described in material and methods. The rates of starch (Vsta), cell wall (Vwall), fatty acids synthesis (Vfas1 and Vfas2) were quantified according to the percentage w/w (Fig. 2B) and the rate of dry weight accumulation. All these fluxes values and their SD's were reported in the model but set as free for the fitting process. The fluxes for amino acid synthesis were estimated by measuring amino acid accumulation in stored proteins during the incubation period and reported as constrained values in the model. The other flux values were calculated from the model based upon carbon enrichment measured after steady-state labeling with 100% [1-¹³C₁]glucose, 100% [1-¹³C₂]glucose or 100% [U-¹³C₅]glutamine. The values are the best fit and also the most frequently determined optimized flux values ± confidence range.

^a Experimentally measured

^b Constrained according to labeling and literature

^c Estimated by label modeling

Table 3 presents a comparison between *in vitro* enzyme activities and *in vivo* fluxes in maize embryo and endosperm tissues. In maize endosperm that mostly accumulates starch, the requirements for reducing power are low and the carbon mainly serves to starch synthesis (Alonso et al., unpublished results). In this tissue, the enzymes of the oxidative pentose phosphate pathway and the malic enzymes are present in large excess in comparison to their fluxes (Table 3). In comparison, maize embryos that produce mainly oil have high demands on reductant and carbon for fatty acid synthesis. The fluxes through the OPPP and the NAD-dependent malic enzyme are not limited by the quantity of their enzyme in maize embryos. Nevertheless, the flux through NADP-dependent malic enzyme is not significantly different from its enzyme activity, suggesting that this enzyme may be limiting (Table 3).

4. Discussion

4.1. Potential limitations of this study

Not all the labeling data was used for fitting experiments. The ¹³C enrichments of free alanine and gamma-aminobutyric acid (GABA; Table 1), and the mass isotopomer abundance of alanine from protein hydrolysis (Supplemental Table 1) were not incorporated into our model. Indeed, the labeling in free alanine and the one in the alanine from protein hydrolysis were inconsistent with the labeling measured in glycerol from triacyl glycerol and in serine, glycine, phenylalanine and tyrosine from protein hydrolysis. The labeling of GABA was significantly different from the labeling of glutamine. These discrepancies are

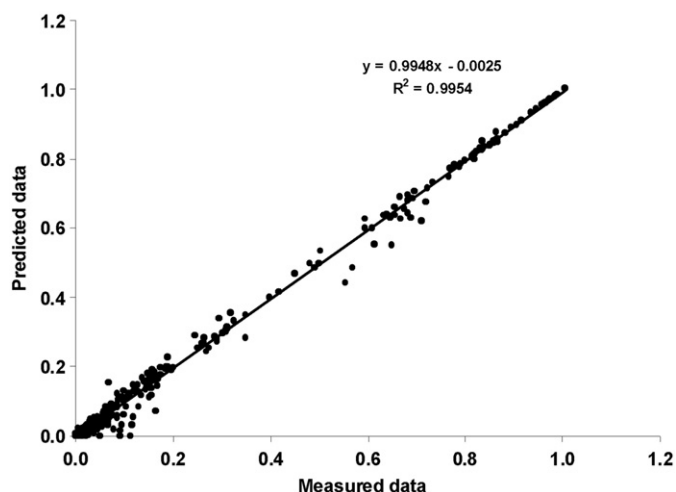


Fig. 4. Comparison between predicted and measured data. Scatter plot between the data calculated by the model and the measurements. The linear regression equation and R^2 value are shown.

Table 3

Comparison of *in vitro* enzyme activities with *in vivo* fluxes in maize embryo and endosperm tissues.

	Maize embryo $\text{nmol h}^{-1} \text{embryo}^{-1}$	Maize endosperm $\text{nmol h}^{-1} \text{endosperm}^{-1}$
<i>In vitro</i> enzyme activities		
Glucose 6-phosphate dehydrogenase	856 ± 201	2071 ± 165
6-phosphogluconate dehydrogenase	1938 ± 377	5263 ± 272
NADP-dependent malic enzyme	175 ± 21	1323 ± 61
NAD-dependent malic enzyme	80 ± 23	95 ± 80
<i>In vivo</i> fluxes		
Vppp1	208 ± 18	$87 \pm 29^*$
Vmep	163 ± 10	$8 \pm 2^*$
Vme	21 ± 8	$12 \pm 10^*$

Enzyme activities were measured on extracts from 22DAP endosperm and germ tissues as described in Material and Methods. *In vivo* flux rates determined by 13C-FLUX are reported for 22DAP embryos and 28DAP endosperms.

* Data extracted from Alonso et al. (unpublished results).

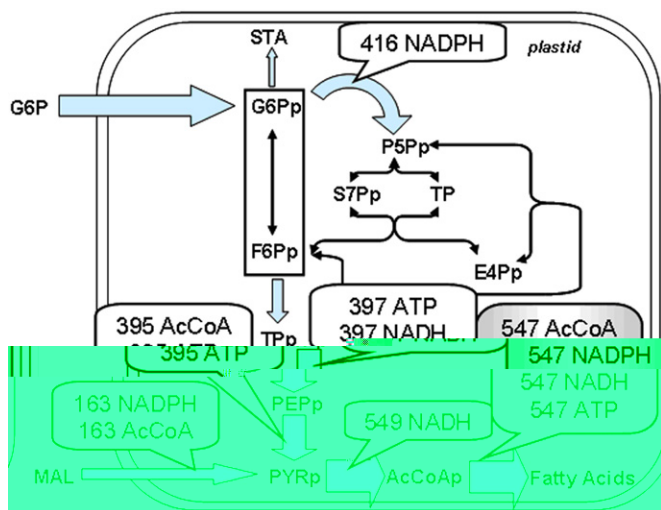


Fig. 5. Source of carbon, reducing power and ATP for fatty acid synthesis. The scheme shown is a simplified overview of the pathways located in the plastid. The blue arrow widths are directly proportional to net flux values. The requirements for fatty acid synthesis are presented in the gray callout, whereas Acetyl-CoA, ATP and reducing power producing steps are presented in white callouts. Units are $\text{nmol molecule h}^{-1} \text{embryo}^{-1}$.

embryos since plastidic glyceraldehyde 3-P dehydrogenase and pyruvate dehydrogenase produce $946 \pm 60 \text{ nmol NADH h}^{-1} \text{embryo}^{-1}$. Only $547 \pm 34 \text{ nmol NADH h}^{-1} \text{embryo}^{-1}$ are required for fatty acid synthesis, which leaves an excess of $399 \text{ nmol NADH h}^{-1} \text{embryo}^{-1}$ in the plastid (Fig. 5). Part of this NADH may be transferred to the cytosol via a plastidic oxalate/malate shuttle (Heineke et al., 1991) and then oxidized in the mitochondria. The NADH potentially translocated from the plastid, together with the NADH produced in the cytosol and the mitochondria, would predict a rate of oxygen consumption of $676 \pm 51 \text{ nmol O}_2 \text{ h}^{-1} \text{embryo}^{-1}$, which is not significantly different from the experimental rate of O_2 consumption.

4.2. Role for plastidic NADP-dependent malic enzyme in fatty acid synthesis

In *Brassica napus* embryos, carbon for fatty acid synthesis was provided by 3-phospho glycerate derived from the ribulose-1, 5-bisphosphate carboxylase oxygenase (RuBisCo) reaction and glycolysis, whereas NADPH and ATP could be largely supplied by light (Table 4; Schwender et al., 2004, 2006; Ruuska et al., 2004; Goffman et al., 2005). Flux through RuBisCo is lower in soybean embryos where 80% of plastidic acetyl CoA is apparently made from triose-P and 20% by malate; reductant and ATP power are partially provided by light (Table 4; Allen et al., 2009a). We have previously demonstrated that developing sunflower embryos, mainly accumulating oil, lost 50% of the carbon uptake as CO_2 (Table 4; Alonso et al., 2007a). The flux map for sunflower embryos revealed that in contrast to findings in green seeds (Schwender et al., 2004, 2006; Allen et al., 2009a) the requirements in ATP and NADPH for fatty acid synthesis were provided by high fluxes through TCA cycle and OPPP, respectively (Table 4), pathways that also release a lot of CO_2 (Alonso et al., 2007a). We measured a higher carbon conversion efficiency of about 80% in developing maize endosperm (Alonso et al., unpublished results). This tissue that mostly produces starch has low ATP and reductant demands and thus, low fluxes through the TCA cycle and OPPP (Table 4). In the present study on maize germs, plastidic NADP-dependent malic enzyme was found to play a key role in supplying carbon and NADPH for fatty acid synthesis, which makes this enzyme an attractive target for

likely to be (Allen, D.K., Ohlrogge, J.B., Shachar-Hill, Y., personal communication) explained by the presence of different pools of alanine and GABA in plant cells but our current methods of extraction do not allow them to be separated. We thus removed the labeling measurements of alanine and GABA from the fitting process.

The fluxes through reactions producing NADH in the cytosol and mitochondria (pyruvate dehydrogenase, isocitrate dehydrogenase, malate dehydrogenase, α -ketoglutarate dehydrogenase, succinate dehydrogenase, malic enzyme and cytosolic glyceraldehyde 3-P dehydrogenase; Fig. 3) estimated by the flux modeling, produce $952 \pm 62 \text{ nmol of NADH h}^{-1} \text{embryo}^{-1}$. Since two moles of NADH are required to reduce one mole of O_2 , the rate of oxygen consumption estimated by the model is $476 \pm 31 \text{ nmol O}_2 \text{ h}^{-1} \text{embryo}^{-1}$. This value is significantly different from the rate of O_2 consumption determined experimentally ($774 \pm 68 \text{ nmol O}_2 \text{ h}^{-1} \text{embryo}^{-1}$; $n=3$). However the flux map indicates that the plastid contributes to a large part of the NADH produced in maize

Table 4
Comparison of seed composition and metabolism.

Tissue	Biomass composition (% w/w)			CCE (%)	Carbon flow (% total carbon uptake)			
	TAG	Protein	Carbohydrates		OPPP	NADP-ME	TCA cycle	RuBisCo
Maize endosperm ^a	1	10	89	80 to 84	12.3	0.8	10.5	0
Soybean embryo ^b	18	38	43	82	< 7.9	< 12.5	6.6	10.2
Maize embryo	34	6	60	57 to 71	36.4	19.0	9.8	0
Sunflower embryo ^c	40	17	44	50	44.8	2.0	37.8	0
Rapeseed embryos ^{d,e}	45	30	25	77 to 86	8.5	0	2.7	24.5

Biomass composition, CCE and percentage of carbon flow were calculated and reported according to

^a Alonso et al. (unpublished results).

^b Allen et al. (2009a).

^c Alonso et al. (2007a).

^d Schwender et al., (2004).

^e Schwender et al., (2006).

engineering compositional changes in maize germ. Furthermore, NADP-dependent malic enzyme has been shown to play an important role in NADPH production in other organisms (Zhang et al., 2007; McKinlay et al., 2007).

There are several isoforms of NADP-dependant malic enzyme in maize (Drincovich et al., 2001). One of the isoforms is found in several C₄ plants and is used for the decarboxylation of malate in bundle sheath chloroplasts; the CO₂ produced is then fixed by RuBisCo (Maurino et al., 1996). A non-photosynthetic isoform of NADP-dependant malic enzyme in plastids of C₄ plants was identified in etiolated leaves and roots of maize (Maurino et al., 1996, 1997, 2001). This isoform represents a protein with a constitutive pattern of expression in plastids of maize and is under transcriptional and post-transcriptional regulation by effectors related to plant defense responses (Maurino et al., 2001). A cytosolic NADP-dependant malic isoform was characterized recently (Detarsio et al., 2008) and its transcripts were found exclusively in embryo and emerging roots. Detarsio et al. (2008) have shown that both plastidic and cytosolic NADP-dependant malic enzyme isoforms are expressed at relatively high levels in embryos from mature seedlings. The plastidic malic enzyme was proposed to be involved in fatty acid synthesis, employing malate as the substrate, as has been demonstrated in *Ricinus communis* (Smith et al., 1992). In oleaginous micro-organisms such as filamentous fungi, lipid accumulation is considered to be controlled by the activity of cytosolic NADP-dependent malic enzyme since it correlates closely with lipid accumulation (Wynn et al., 1999; Ratledge, 2002). Doehlert and Lambert (1991) have shown that oil concentrations in kernels of maize genotypes with widely divergent chemical composition were positively correlated with mature embryo dry weights and with malic enzyme activities in isolated embryos harvested at 20DAP. Our study not only points out a key role for plastidic NADP-dependant malic enzyme activity in supplying carbon and reductant for fatty acid synthesis in developing maize embryos (Table 4) but also demonstrates that the flux through this enzyme is limited by its quantity (Table 3).

Acknowledgments

We are grateful to the Calgene greenhouse staff (Dan Ovaday and Adela Contreras) for corn production, Maureen Daley and Bihua Huang (Monsanto) for assistance with tissue cultures, Prof. Randy Beaudry (MSU) for help with determining gas compositions, Beverly Chamberlin of the MSU GC-MS facility, Daniel Holmes of the MSU NMR facility, Hart Poskar for software, Russell LaClair and Rebecca Piasecki (MSU) for technical help, the Monsanto crop analytics team (Mary Mierkowski, Wayne Brown and Ron Colletti) in St. Louis for amino acid analysis.

Appendix A. Supplementary material

Supplementary data associated with this article can be found in the online version at doi:10.1016/j.ymben.2010.04.002.

References

- Allen, D.K., Ohlrogge, J.B., Shachar-Hill, Y., 2009a. The role of light in soybean seed filling metabolism. *Plant J.* 58 (2), 220–234.
- Allen, D.K., Ohlrogge, J.B., Shachar-Hill, Y., 2009b. Metabolic flux analysis in plants: coping with complexity. *Plant Cell Environ.* 32 (9), 1241–1257.
- Alonso, A.P., Vigeolas, H., Raymond, P., Rolin, D., Dieuaide-Noubhani, M., 2005. A new substrate cycle in plants. Evidence for a high glucose-phosphate-to-glucose turnover from *in vivo* steady-state and pulse-labeling experiments with [C-13] glucose and [C-14] glucose. *Plant Physiol.* 138, 2220–2232.
- Alonso, A.P., Goffman, F.D., Ohlrogge, J.B., Shachar-Hill, Y., 2007a. Carbon conversion efficiency and central metabolic fluxes in developing sunflower (*Helianthus annuus* L.) embryos. *Plant J.* 52 (2), 296–308.
- Alonso, A.P., Raymond, P., Hernould, M., Rondeau-Mouro, C., de Graaf, A., Chourey, P., Lahaye, M., Shachar-Hill, Y., Rolin, D., Dieuaide-Noubhani, M., 2007b. A metabolic flux analysis to study the role of sucrose synthase in the regulation of the carbon partitioning in central metabolism in maize root tips. *Metab. Eng.* 9 (5–6), 419–432.
- Alonso, A.P., Val, D.L., Shachar-Hill, Y. Central metabolic fluxes in the endosperm of developing maize seeds and their implications for metabolic engineering. *Phytochemistry*, unpublished results.
- Boyle, S.A., Hemmingsen, S.M., Dennis, D.T., 1990. Energy requirement for the import of proteins from developing endosperm of *Ricinus communis* L. *Plant Physiol.* 92, 151–154.
- Browse, J., Slack, C.R., 1985. Fatty-acid synthesis in plastids from maturing safflower and linseed cotyledons. *Planta* 166, 74–80.
- Detarsio, E., Maurino, V.G., Alvarez, C.E., Müller, G.L., Andreo, C.S., Drincovich, M.F., 2008. Maize cytosolic NADP-malic enzyme (ZmCytNADP-ME): a phylogenetically distant isoform specifically expressed in embryo and emerging roots. *Plant Mol. Biol.* 68, 355–367.
- Dieuaide-Noubhani, M., Alonso, A.P., Rolin, D., Eisenreich, W., Raymond, P., 2007. Metabolic flux analysis: recent advances in carbon metabolism in plants. *EXS* 97, 213–243.
- Dieuaide-Noubhani, M., Raffard, G., Canioni, P., Pradet, A., Raymond, P., 1995. Quantification of compartmented metabolic fluxes in maize root tips using isotope distribution from 13C- or 14C-labeled glucose. *J. Biol. Chem.* 270, 13147–13159.
- Doehlert, D.C., Lambert, R.J., 1991. Metabolic characteristics associated with starch, protein, and oil deposition in developing maize kernels. *Crop Sci.* 31 (1), 151–157.
- Drincovich, M.F., Casati, P., Andreo, C.S., 2001. NADP-malic enzyme from plants: a ubiquitous enzyme involved in different metabolic pathways. *FEBS Lett.* 490, 1–6.
- Eastmond, P.J., Rawsthorne, S., 2000. Coordinate changes in carbon partitioning and plastidial metabolism during the development of oilseed rape embryo. *Plant Physiol.* 122, 767–774.
- Ettenhuber, C., Spielbauer, G., Margl, L., Hannah, L.C., Gierl, A., Bacher, A., Genschel, U., Eisenreich, W., 2005. Changes in flux pattern of the central carbohydrate metabolism during kernel development in maize. *Phytochemistry* 66 (22), 2632–2642.
- Fuhrmann, J., Johnen, T., Heise, K.P., 1994. Compartmentation of fatty acid metabolism in zygotic rape embryos. *J. Plant Physiol.* 143, 565–569.
- Glawischnig, E., Gierl, A., Tomas, A., Bacher, A., Eisenreich, W., 2001. Retrosynthetic nuclear magnetic resonance analysis of amino acid biosynthesis

- and intermediary metabolism. Metabolic flux in developing maize kernels. *Plant Physiol.* 125 (3), 1178–1186.
- Glawischig, E., Gierl, A., Tomas, A., Bacher, A., Eisenreich, W., 2002. Starch biosynthesis and intermediary metabolism in maize kernels. Quantitative analysis of metabolite flux by nuclear magnetic resonance. *Plant Physiol.* 130 (4), 1717–1727.
- Goffman, F.D., Alonso, A.P., Schwender, J., Shachar-Hill, Y., Ohlrogge, J.B., 2005. Light enables a very high efficiency of carbon storage in developing embryos of rapeseed. *Plant Physiol.* 138, 2269–2279.
- Heineke, D., Riens, B., Grosse, H., Hoferichter, P., Peter, U., Flügge, U.I., Heldt, H.W., 1991. Redox transfer across the inner chloroplast envelope membrane. *Plant Physiol.* 95, 1131–1137.
- Hill, L.M., Smith, A.M., 1991. Evidence that glucose-6-phosphate is imported as the substrate for starch synthesis by the plastids of developing pea embryos. *Planta* 185, 91–96.
- Kang, F., Rawsthorne, S., 1994. Starch and fatty acid synthesis in plastids from developing embryos of oilseed rape (*Brassica napus* L.). *Plant J.* 6, 795–805.
- Kang, F., Rawsthorne, S., 1996. Metabolism of glucose-6-phosphate and utilization of multiple metabolites for fatty acid synthesis by plastids from developing oilseed rape embryos. *Planta* 199, 321–327.
- Kleppinger-Sparace, K.F., Stahl, R.J., Sparace, S.A., 1992. Energy-requirements for fatty-acid and glycerolipid biosynthesis from acetate by isolated pea root plastids. *Plant Physiol.* 98, 723–727.
- Libourel, I.G.L., Gehan, J.P., Shachar-Hill, Y., 2007. Design of substrate label for steady state flux measurements in plant systems using metabolic network of *Brassica napus* embryos. *Phytochemistry* 68, 2211–2221.
- Libourel, I.G.L., Shachar-Hill, Y., 2008. Metabolic flux analysis in plant: from intelligent design to rational engineering. *Annu. Rev. Plant Biol.* 59, 625–650.
- Lonien, J., Schwender, J., 2009. Analysis of metabolic flux phenotypes for two *Arabidopsis* mutants with severe impairment in seed storage lipid synthesis. *Plant Physiol.* 151 (3), 1617–1634.
- Maurino, V.G., Drincovich, M.F., Andreo, C.S., 1996. NADP-malic enzyme isoforms in maize leaves. *Biochem. Mol. Biol. Int.* 38, 239–250.
- Maurino, V.G., Drincovich, M.F., Casati, P., Andreo, C.S., Ku, M.S.B., Gupta, S.K., Edwards, G.E., Franceschi, V.R., 1997. NADP-malic enzyme: immunolocalization in different tissues of the C₄ plant maize and the C₃ plant wheat. *J. Exp. Bot.* 48, 799–811.
- Maurino, V.G., Saigo, M., Andreo, C.S., Drincovich, M.F., 2001. Non-photosynthetic malic enzyme from maize: a constitutively expressed enzyme that responds to plant defence inducers. *Plant Mol. Biol.* 45, 409–420.
- McKinlay, J.B., Shachar-Hill, Y., Zeikus, J.G., Vieille, C., 2007. Determining *Actinobacillus succinogenes* metabolic pathways and fluxes by NMR and GC-MS analyses of ¹³C-labeled metabolic product isotopomers. *Metab. Eng.* 9 (2), 177–192.
- Möhlmann, T., Scheibe, R., Neuhaus, H.E., 1994. Interaction between starch synthesis and fatty acid synthesis in isolated cauliflower-bud amyloplasts. *Planta* 194, 492–497.
- Moing, A., Escobar-Gutierrez, A., Gaudillere, J.P., 1994. Modeling carbon export out of mature peach leaves. *Plant Physiol.* 106, 591–600.
- Möllney, M., Wiechert, W., Kownatzki, D., de Graaf, A.A., 1999. Bidirectional reaction steps in metabolic networks: IV. Optimal design of isotopomer labeling experiments. *Biotechnol. Bioeng.* 66, 86–103.
- Neuhaus, H.E., Emes, M.J., 2000. Nonphotosynthetic metabolism in plastids. *Annu. Rev. Plant Physiol. Mol. Biol.* 51, 111–140.
- Neuhaus, H.E., Batz, O., Thom, E., Scheibe, R., 1993. Purification of highly intact plastids from various heterotrophic plant-tissues. Analysis of enzymatic equipment and precursor dependency for starch biosynthesis. *Biochem. J.* 296, 395–401.
- Pleite, R., Pike, M.J., Garces, R., Martinez-Force, E., Rawsthorne, S., 2005. The sources of carbon and reducing power for fatty acid synthesis in the heterotrophic plastids of developing sunflower (*Helianthus annuus* L.) embryos. *J. Exp. Bot.* 56, 1297–1303.
- Porter, G.A., Kniewel, D.P., Shannon, J.C., 1985. Sugar efflux from maize (*Zea mays* L.) pedicel tissue. *Plant Physiol.* 77 (3), 524–531.
- Porter, G.A., Kniewel, D.P., Shannon, J.C., 1987. Assimilate unloading from maize (*Zea mays* L.) pedicel tissues. II. Effects of chemical agents on sugar, amino acid, and ¹⁴C-assimilate unloading. *Plant Physiol.* 85, 558–565.
- Qi, Q., Kleppinger-Sparace, K.F., Sparace, S.A., 1994. The role of the triose-phosphate shuttle and glycolytic intermediates in fatty acid and glycerolipid biosynthesis in pea root plastids. *Planta* 194, 193–199.
- Qi, Q.G., Kleppinger-Sparace, K.F., Sparace, S.A., 1995. The utilization of glycolytic-intermediates as precursors for fatty-acid biosynthesis by pea root plastids. *Plant Physiol.* 107, 413–419.
- Ratcliffe, R.G., Shachar-Hill, Y., 2005. Revealing metabolic phenotypes in plants: inputs from NMR analysis. *Biol. Rev.* 80, 27–43.
- Ratcliffe, R.G., Shachar-Hill, Y., 2006. Measuring multiple fluxes through plant metabolic networks. *Plant J.* 45, 490–511.
- Ratledge, C., 2002. Regulation of lipid accumulation in oleaginous microorganisms. *Biochem. Soc. Trans.* 30, 1047–1050.
- Rawsthorne, S., 2002. Carbon flux and fatty acid synthesis in plants. *Prog. Lipid Res.* 41, 182–196.
- Rontein, D., Dieuaide-Noubhani, M., Dufourc, E.J., Raymond, P., Rolin, D., 2002. The metabolic architecture of plant cells. Stability of central metabolism and flexibility of anabolic pathways during the growth cycle of tomato cells. *J. Biol. Chem.* 277, 43948–43960.
- Roughan, P.G., Holland, R., Slack, C.R., 1979. Control of long-chain fatty acid synthesis in isolated intact spinach (*Spinacia-Oleracea*) chloroplasts. *Biochem. J.* 184, 193–202.
- Ruuska, S.A., Schwender, J., Ohlrogge, J.B., 2004. The capacity of green oilseeds to utilize photosynthesis to drive biosynthetic processes. *Plant Physiol.* 136, 2700–2709.
- Schuster, R., 1988. Determination of amino acids in biological, pharmaceutical, plant and food samples by automated precolumn derivatization and HPLC. *J. Chromatogr.* 431, 271–284.
- Schwender, J., Ohlrogge, J.B., Shachar-Hill, Y., 2003. A flux model of glycolysis and the oxidative pentosephosphate pathway in developing *Brassica napus* embryos. *J. Biol. Chem.* 278, 29442–29453.
- Schwender, J., Goffman, F., Ohlrogge, J.B., Shachar-Hill, Y., 2004. Rubisco without the Calvin cycle improves the carbon efficiency of developing green seeds. *Nature* 432, 779–782.
- Schwender, J., Shachar-Hill, Y., Ohlrogge, J.B., 2006. Mitochondrial metabolism in developing embryos of *Brassica napus*. *J. Biol. Chem.* 281, 34040–34047.
- Smith, R.G., Gauthier, D.A., Dennis, D.T., Turpin, D.H., 1992. Malate-dependent and pyruvate-dependent fatty-acid synthesis in leukoplasts from developing castor endosperm. *Plant Physiol.* 98, 1233–1238.
- Spielbauer, G., Margl, L., Hannah, L.C., Römisch, W., Ettenhuber, C., Bacher, A., Gierl, A., Eisenreich, W., Genschel, U., 2006. Robustness of central carbohydrate metabolism in developing maize kernels. *Phytochemistry* 67 (14), 1460–1475.
- Sriram, G., Fulton, D.B., Iyer, V.V., Peterson, J.M., Zhou, R.L., Westgate, M.E., Spalding, M.H., Shanks, J.V., 2004. Quantification of compartmented metabolic fluxes in developing soybean embryos by employing Biosynthetic ally directed fractional C-13 labeling, [C-13, H-1] two-dimensional nuclear magnetic resonance, and comprehensive isotopomer balancing. *Plant Physiol.* 136, 3043–3057.
- Weaire, P.J., Kekwick, R.G.O., 1975. Fractionation of fatty-acid synthetase activities of avocado mesocarp plastids. *Biochem. J.* 146, 439–445.
- Wiechert, W., de Graaf, A.A., 1997. Bidirectional reaction steps in metabolic networks .1. Modeling and simulation of carbon isotope labeling experiments. *Biotechnol. Bioeng.* 55, 101–117.
- Wiechert, W., Siefke, C., de Graaf, A.A., Marx, A., 1997. Bidirectional reaction steps in metabolic networks .2. Flux estimation and statistical analysis. *Biotechnol. Bioeng.* 55, 118–135.
- Wiechert, W., Möllney, M., Isermann, N., Wurzel, W., de Graaf, A.A., 1999. Bidirectional reaction steps in metabolic networks: III. Explicit solution and analysis of isotopomer labeling systems. *Biotechnol. Bioeng.* 66, 69–85.
- Wiechert, W., Möllney, M., Petersen, S., de Graaf, A.A., 2001. A universal framework for C-13 metabolic flux analysis. *Met. Eng.* 3, 265–283.
- Williams, T.C.R., Miguelt, L., Masakapalli, S.K., Kruger, N.J., Sweetlove, L.J., Ratcliffe, R.G., 2008. Metabolic network fluxes in heterotrophic *Arabidopsis* cells: stability of the flux distribution under different oxygenation conditions. *Plant Physiol.* 148, 704–718.
- Wynn, J.P., Hamid, A.B.A., Ratledge, C., 1999. The role of malic enzyme in the regulation of lipid accumulation in filamentous fungi. *Microbiology* 145, 1911–1917.
- Zhang, Y., Adams, I.P., Ratledge, C., 2007. Malic enzyme: the controlling activity for lipid production? Overexpression of malic enzyme in *Mucor circinelloides* leads to a 2.5-fold increase in lipid accumulation. *Microbiology* 153 (7), 2013–2025.